Biophysical Chemistry 121 (2006) 57 – 64

Biophysical Chemistry

http://www.elsevier.com/locate/biophyschem

# Influence of spectral heterogeneity of prodan and laurdan solutions on the transfer of electronic energy to octadecyl rhodamine B

K.A. Kozyra [a,b,*], J.R. Heldt [a], J. Heldt [a]

[a] *Institute of Experimental Physics, University of Gdańsk, Wita Stwosza 57, 80-952 Gdańsk, Poland*
[b] *Institute of Physics and Biophysics, Department of Food Science, University of Warmia and Mazury, Oczapowskiego 4, 10-900 Olsztyn, Poland*

Received 25 May 2005; received in revised form 24 November 2005; accepted 25 November 2005

**Abstract**

Fluorescence quenching and resonance energy transfer have been studied by steady-state fluorescence spectroscopy. The experimental and theoretical values for the rate constants of the electronic energy transfer ($k_{ET}$) and critical radius ($R_0$) were determined for prodan and laurdan as donors and octadecyl rhodamine B as acceptor. The spectroscopic data show, that prodan and laurdan in solution create an inhomogeneous spectroscopic medium in which multi-channel luminescence phenomena take place. This finding indicated that the modified form of the Stern–Volmer relation should be used for analyzing fluorescence quenching data. Results of performed studies point out, that dipole–dipole interaction is responsible for the resonance energy transfer from prodan and laurdan to octadecyl rhodamine B. The relative quenching efficiencies of both dyes depend on polarity of the medium and are higher for more polar solvent (AcN).

*Keywords:* Prodan; Laurdan; Fluorescence quenching; Heterogeneously emitting systems; Energy transfer

## 1. Introduction

The quenching of fluorescence caused by the resonance energy transfer from electronically excited donor molecule, $D^*$, to an acceptor molecule, $A$, which becomes excited to a higher electronic state, is a widely studied phenomenon [1–4]. The studies of energy transfer have both theoretical as well as practical importance. This phenomenon has found applications in many fields including the photochemistry for elucidating mechanisms of photochemical reactions [5] and has been effectively used as a spectroscopic ruler in a wide variety of biological macromolecules and assemblies [2,3,6]. Furthermore, energy transfer is a key step in biologically important processes such as the photosynthetic process in plants [7].

The quenching of fluorescence requires a close approach of fluorophore and quencher, and usually is interpreted according to theories assuming either dynamic or static quenching, or a combination of both [6]. The Stern–Volmer theory has been applied successfully to a wide variety of quenching studies in isotropic and low-viscosity solutions. When a system contains a fluorophore in different environments (e.g. a fluorophore embedded in microheterogeneous materials as sol–gel matrices, polymers, etc.) or more than one fluorophore (e.g. different tryptophanyl residues of a protein), the classical Stern–Volmer theory cannot be applied. A proper treatment of quenching processes in heterogeneously emitting systems requires additional considerations [1,2,10].

In this paper we focus besides the spectral properties of prodan (6-propionyl-2-dimethylaminonaphtalene) and laurdan (6-dodecanoyl-2-dimethylaminonaphtalene), the quenching of their excited states by octadecyl rhodamine B (ORB) (shown on Scheme 1). A particular attention has been paid to these organic molecules since they are capable of simultaneous creation of locally excited $S_1$(LE) and charge transfer $S_1$(CT) excited states [11–16]. As it has been shown in a series of our previous papers [13–16], the solutions of prodan and laurdan in neat solvents and phospholipid vesicles are spectrally an inhomogeneous system in which multi-channel luminescence phenomena take place. The spectroscopic heterogeneity is due to distribution of space conformational forms possessing different twisting angles $\varphi$ between the mutual orientation

---

[*] Corresponding author. Tel./fax: +48 895233406.
*E-mail address:* katarzyna.kozyra@uwm.edu.pl (K.A. Kozyra).

0301-4622/$ - see front matter © 2005 Elsevier B.V. All rights reserved.
doi:10.1016/j.bpc.2005.11.009

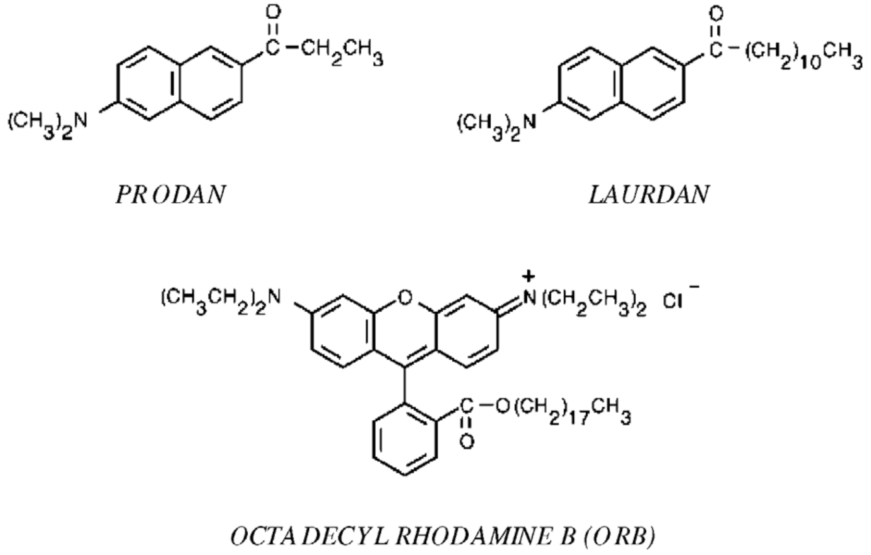

Scheme 1. Chemical structure of donor (prodan, laurdan) and acceptor (octadecyl rhodamine B) molecules.

planes of the dimethyl group ($-N(CH_3)_2$) and the naphthalene moiety, and by accompanying intra- and intermolecular charge transfer phenomena.

In the following, we report results of performed intermolecular electronic energy transfer studies in isotropic solutions of the heterogeneously emitting systems. A special attention has been paid to the description of the fluorescence quenching occurring in the heterogeneously emitting systems.

## 2. Experimental details

Prodan, laurdan and ORB were purchased from Molecular Probes (Eugene, OR) and used without further purification. The solvents tetrahydrofuran (THF) and acetonitrile (AcN) were of spectroscopic grade and provided by Merck (Darmstadt, Germany).

The absorption spectra of the dyes were measured on Shimadzu UV-2401 PC spectrophotometer. The fluorescence spectra of the compounds and their mixtures were carried out with a Shimadzu RF-5301 spectrofluorometer. Fluorescence quenching measurements were performed using triangular cuvette with frontal excitation to minimize the effect of reabsorption of donor emission by the acceptor. The emission was observed perpendicular to the direction of the exciting beam. Thus, the errors due to fluorescence reabsorption were reduced in a way that mathematical corrections were superfluous.

The fluorescence lifetime measurements were performed by means of the Time Correlated Single Photon Counting Technique (TCSPC). The experimental set up for the performed time resolved measurements has been described elsewhere [16,17].

The quantum yield, $\Phi_F$, was determined by comparison with a standard solution using β-carboline in 1 N sulphuric acid as a reference compound [6,18]. The value of quantum yield of the used standard solution is equal $\Phi_F{}^S = 0.6$ [6].

## 3. Results and discussion

### 3.1. Spectral properties of one compound solution

In Fig. 1 the emission spectra of prodan and laurdan in THF and AcN are reported. As expected for a dye molecule containing a donor and acceptor groups, its emission is dependent on the polarity of the environment. As can be seen on Fig. 1, the emission maxima of prodan and laurdan in THF are 431 and 432 nm. While those values are considerably red shifted in AcN, and equal 456 and 452 nm, respectively. The preceding of experimental observation [14–16] agree with the results of the quantum mechanical calculations [12,13] which predict the existence of $S_1$(LE) and $S_1$(CT) states. The fluorescence spectra of prodan and laurdan obtained in our studies (see Fig. 1), as well as by other authors [11–16] show that the emission of both molecules arises from two different excited states. As it is seen on Fig. 1, the emission spectra of both dyes can be decomposed into two separated bands (Fig. 2) which correspond to the emission arising from either $S_1$(LE) or $S_1$(CT) states. From the decomposition of the fluorescence spectrum into the separated Gaussian bands, we establish the $\lambda_{max}$ value of the LE and CT bands and their half width. We found that the two bands participate in the fluorescence spectrum at the ratio: 1 : 4.8 (THF) and 1 : 1.4 (AcN) for prodan, and 1 : 2 (THF) and 1 : 2.2 (AcN) for laurdan. In conclusion, the number of molecules with changed structural conformation emitting from the $S_1$(CT) state depends on the solvent polarity.

As can be seen from Fig. 2, the absorption spectra of prodan in THF and AcN at room temperature are similar, indicating that the ground states of this compound in the two solvents are identical. The same results were obtained for laurdan molecules (data not shown). Furthermore, the overlap between the donor (prodan and laurdan) emission and acceptor (ORB) absorption spectra is noted. It points to the fact that the donor–acceptor energy transfer can take place in the studied systems: prodan-ORB and laurdan-ORB.

### 3.2. Fluorescence decay times

The fluorescence decays of prodan and laurdan were measured using a fixed excitation wavelength ($\lambda_{exc}=403$ nm) at the magic angle. A satisfactory agreement between the measured fluorescence decay curve and theoretical fitting function has been obtained using multi-exponential function $F(t)=\sum_{i=1}^{n} A_i \exp(-t/\tau_i)$, where $A_i$ and $\tau_i$ are the preexponential coefficient and decay time of $i$-th component, respectively. The fluorescence decays can be well described using a three-exponential model for both dyes, notwithstanding a very short component ($\tau_1 \approx 0.2$ ns) was always obtained with a negative preexponential factor. This negative amplitude indicates that before the radiative deexcitation of an assemble of molecules, a fast reaction compared to the emission lifetime exists, leading to an increase in the emitting population observed by fluorescence. The results of the analysis of the fluorescence decay curve for prodan and laurdan in THF and AcN at room temperature are presented in Table 1. The two longer decays components, described by the $\tau_2$ and $\tau_3$ values, are attributed to the radiative deexcitation of $S_1$(LE) and $S_1$(CT) states, respectively. The values of preexponential coefficients $A_2$, ascribing participation of the decay component of the LE fluorescence band, are greater in THF, than in AcN. On the other hand, the values of $A_3$ are related to CT emission of space conformers of prodan and laurdan. The number of CT conformers increases with increasing polarity of the solvent. This regularity was observed for both molecules under study and has its confirmation in measured fluorescence spectra. The above findings point out that prodan and laurdan solutions in THF and AcN create a heterogeneously emitting system, which fluorescence, we suppose, will be quenched in a complex manner.

### 3.3. Fluorescence quenching

Fig. 3 shows the fluorescence spectra of the donor (prodan and laurdan) obtained in the presence of acceptor (ORB) molecule at its various concentrations in THF. The spectra have been obtained at the donor constant concentration ($C_D=5\times10^{-5}$ M) and for acceptor concentration changes from 0 to $2.5\times10^{-4}$ M. From these spectra it is obvious that with increasing the acceptor concentration a successive decrease occurs in the donor fluorescence intensity. The same dependence (not shown

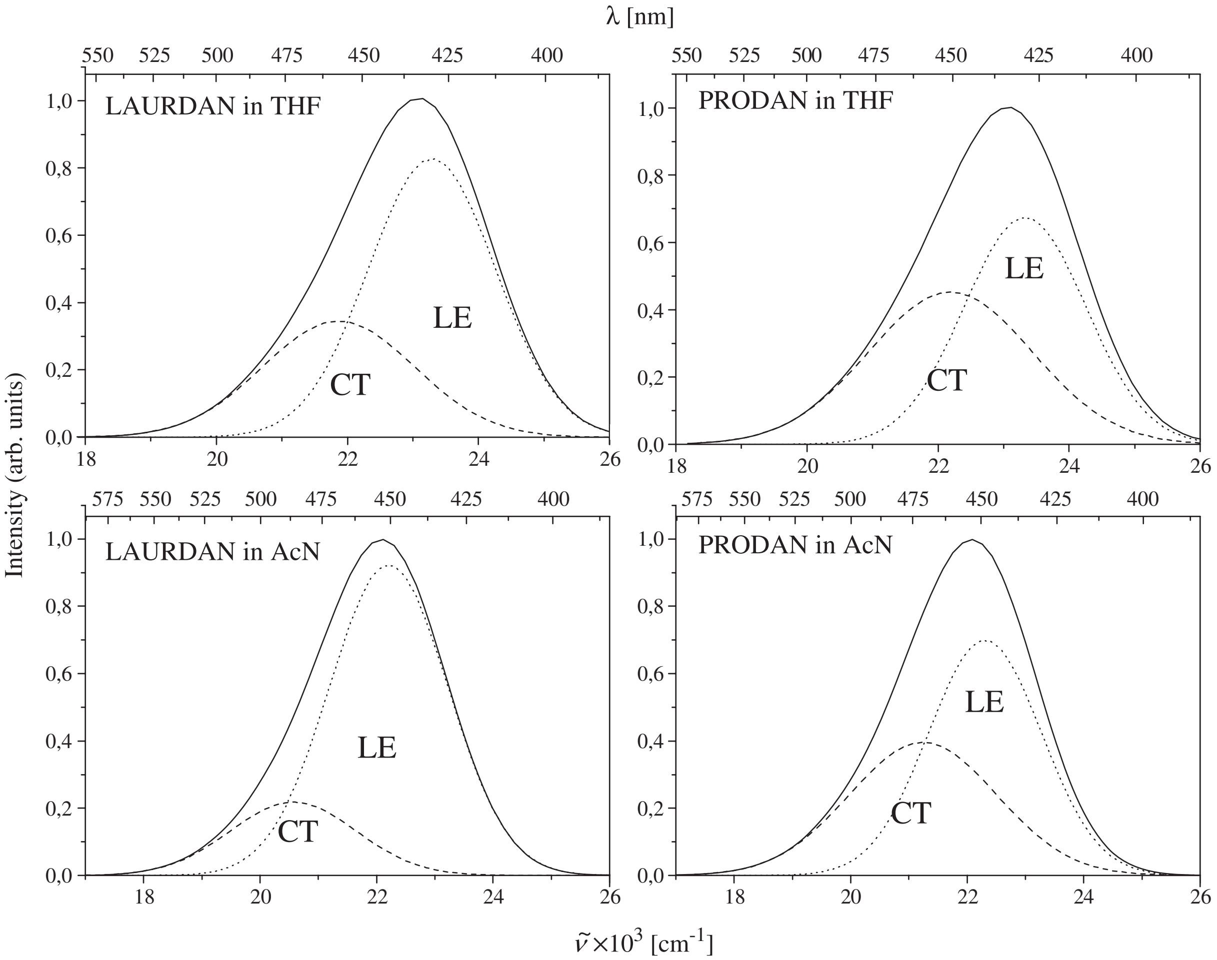

Fig. 1. Emission spectra of prodan and laurdan in THF and AcN and their decomposition on two Gaussian bands corresponding to the emission of molecules from the $S_1$(LE) and $S_1$(CT) states.

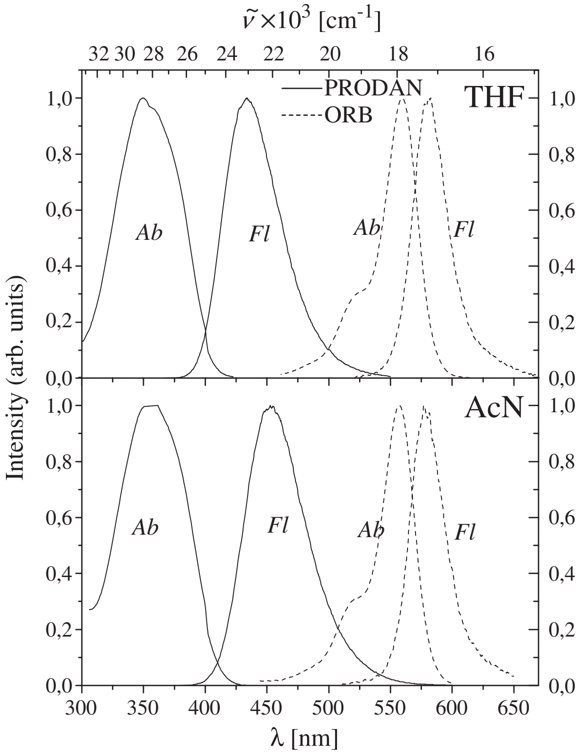

Fig. 2. Normalized fluorescence and absorption spectra of prodan and ORB in THF and AcN.

graphically) is noted for donor–acceptor pairs in AcN. It should be noted that we did not detect any extra absorption band in the spectral range 200–600 nm for the investigated systems. It points to the absence of any detectable ground–state complexes of the donor–acceptor pairs in the solution.

Analyzing the emission spectra of prodan-ORB pair a blue shift of the donor fluorescence spectrum is observed with increasing acceptor concentration. The observed shift is about 3 nm by concentration changes of ORB from $5\times10^{-6}$ to $2.5\times10^{-4}$ M. This finding can be attributable to the radiative transfer phenomena [22]. It is known that the acceptor molecules quench the longer wavelength portion of donor fluorescence spectrum more effectively than the shorter one, whereas the simultaneous successive red shift of laurdan fluorescence maximum can be attributed to reabsorption and radiative migration [22,23]. It results because by the absorption depth of about 2 mm the reabsorption is not completely reduced.

In Fig. 4A, we show plots of prodan and laurdan fluorescence intensity ratio against ORB concentration in physically homogenous solution of THF and AcN. As can be seen on Fig. 4A, the plots are linear for both dyes. Fitting the experimental data to Stern–Volmer equation [8], $K_{\mathrm{SV}}$ values and energy transfer rate constant, $k_{\mathrm{ET}}$, have been calculated. The obtained $k_{\mathrm{ET}}$ values comprise $1.86\times10^{12}$–$4.80\times10^{12}$ l mol$^{-1}$ s$^{-1}$, which is substantially higher than that noted for the bimolecular rate constants controlled by diffusion. Diffusion rate constants have been calculated according to Debye equation [9], and for THF and AcN they are $k_{\mathrm{DIFF}}^{\mathrm{THF}}=2.7\times10^{10}$ l mol$^{-1}$ s$^{-1}$ and $k_{\mathrm{DIFF}}^{\mathrm{AcN}}=2\times10^{10}$ l mol$^{-1}$ s$^{-1}$, respectively. The two order differences noted between $k_{\mathrm{ET}}$ and $k_{\mathrm{DIFF}}$ values indicate a diffusion-free mechanism for the electron energy transfer of the studied D–A pairs.

In order to state the type of the quenching mechanism, the fluorescence decay times for both systems, e.g., prodan-ORB and laurdan-ORB in THF and AcN, were measured as function of acceptor concentration. In those cases, the experimental decay curves were fitted by a three-exponential function, also. The obtained data for prodan-ORB system in THF are graphically presented on Fig. 4B. As can be seen, the $\langle\tau_0\rangle/\langle\tau\rangle$ ratio is independent on acceptor concentration in the errors limit of $\tau$ determination. The same dependence was observed for all systems under study. Therefore, we can ascertain that character of quenching is static.

On the basis of those and our earlier measurements [13–16] and additionally performed measurements of fluorescence decay times (collected in Table 1), it is evident that both prodan and laurdan in used solution form an inhomogeneous spectroscopic medium. Taking this into account, it is obvious that the modified form of the Stern–Volmer relation should be used for analyzing fluorescence quenching data [1,2,19]. If we denote two emitting forms as LE and CT, the quantitative expression for the relation between fluorescence intensity and quencher concentration $[Q]$ is given by the following equation [1,2,19]:

$$\frac{I}{I_0}=\frac{f_{\mathrm{LE}}}{1+K_{\mathrm{SV}}^{\mathrm{LE}}[Q]}+\frac{f_{\mathrm{CT}}}{1+K_{\mathrm{SV}}^{\mathrm{CT}}[Q]}=\frac{f_{\mathrm{LE}}}{1+\tau_{\mathrm{D}}^{\mathrm{LE}}k_{\mathrm{ET}}^{\mathrm{LE}}[Q]}+\frac{f_{\mathrm{CT}}}{1+\tau_{\mathrm{D}}^{\mathrm{CT}}k_{\mathrm{ET}}^{\mathrm{CT}}[Q]},\tag{1}$$

where $I_0$ and $I$ denote the total fluorescence intensities of a fluorophore in the absence and presence of the quencher,

Table 1
Fluorescence decay times of prodan and laurdan in THF and AcN

| Solvent | | Prodan $\lambda_{\mathrm{em}}$=460 nm | | | | Laurdan $\lambda_{\mathrm{em}}$=460 nm | | | |
|---|---|---|---|---|---|---|---|---|---|
| | | $\tau_i$ [ns] | $A_i$ [%] | $\langle\tau\rangle$* | $\chi^2$ | $\tau_i$ [ns] | $A_i$ [%] | $\langle\tau\rangle$* | $\chi^2$ |
| THF | $\tau_1$ | 0.18 | −19,887 (3%) | 3.16 | 1.34 | 0.18 | −23,653 (4%) | 2.78 | 1.53 |
| | $\tau_2$ | 3.09 | 36,499 (90%) | | | 2.40 | 32,287 (66%) | | |
| | $\tau_3$ | 5.46 | 1540 (7%) | | | 3.93 | 9078 (30%) | | |
| AcN | $\tau_1$ | 0.17 | −30,303 (5%) | 2.5 | 1.46 | 0.19 | −30,572 (6%) | 2.32 | 1.32 |
| | $\tau_2$ | 1.98 | 29,386 (60%) | | | 1.75 | 31,200 (59%) | | |
| | $\tau_3$ | 3.84 | 8698 (35%) | | | 3.68 | 8698 (35%) | | |

* Calculated according to: $\langle\tau\rangle=\sum_{i=1}^{n}A_i\tau_i^2/\sum_{i=1}^{n}A_i\tau_i$ [6].

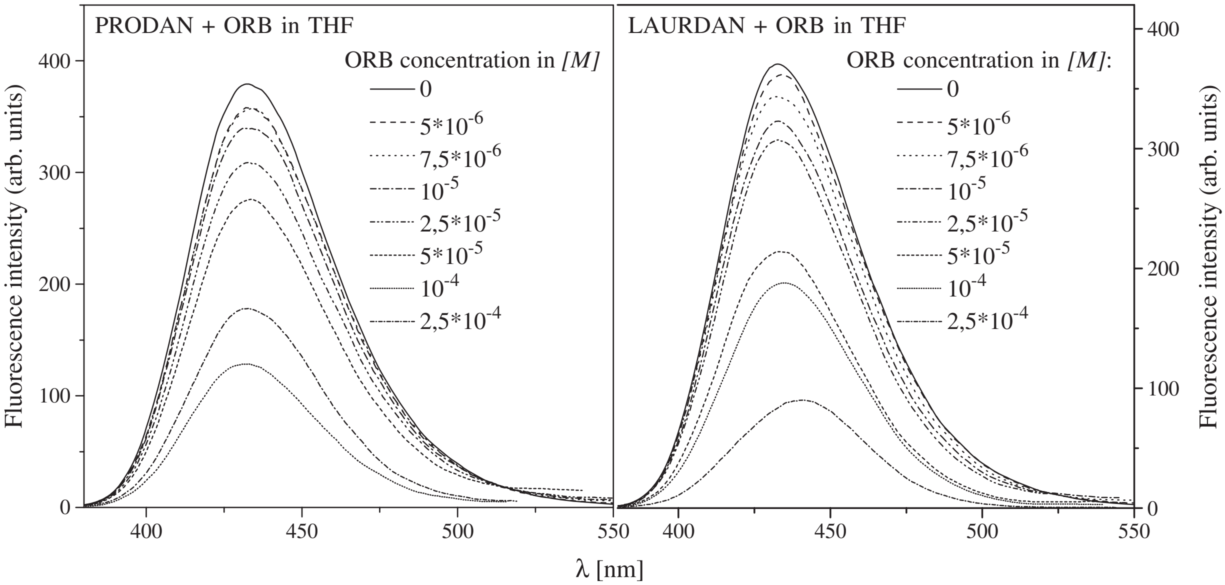

Fig. 3. Emission spectra of prodan and laurdan in THF in the presence of various concentration of ORB.

respectively. $f_{LE}$ and $f_{CT}$ are the fractional contributions of the emitting forms to the total fluorescence intensity, $K_{SV}^{LE}$, $K_{SV}^{CT}$, $\tau_D^{LE}$ and $\tau_D^{CT}$ are the Stern–Volmer constants and decay times of emitting forms, respectively.

The fitting of experimental data to Eq. (1) was performed by using a non-linear least-squares procedure (ORIGIN 7.0). As a result of performed calculations the values of $K_{SV}^{LE}$, $K_{SV}^{CT}$, $f_{LE}$ and $f_{CT}$ were obtained. Using the Stern–Volmer constants and decay times, the energy transfer rate constants for prodan and laurdan molecules emitting from $S_1$(LE) and $S_1$(CT) states were calculated. The results are listed in Table 2. An accurate analysis of the parameters describing the fluorescence quenching of the studied D–A pairs indicates that:

- the values of $k_{ET}^{LE}$ and $k_{ET}^{CT}$ of prodan-ORB and laurdan-ORB systems comprise $2.05\times10^{12}$–$6.06\times10^{12}$ l mol$^{-1}$ s$^{-1}$, and are greater than the bimolecular rate constants controlled by diffusion for both, THF and AcN, $k_{DIFF}^{THF}=2.7\times10^{10}$ l mol$^{-1}$ s$^{-1}$ and $k_{DIFF}^{AcN}=2\times10^{10}$ l mol$^{-1}$ s$^{-1}$.
- the fluorescence quenching rate constants determined for laurdan-ORB system are greater than for pair prodan-ORB, and implement the relation $k_{ET}$(AcN)>$k_{ET}$(THF), i.e., the values are higher for more polar solvent.
- the fluorescence of prodan and laurdan is quenched by ORB with greater probability, if the emission arises from $S_1$(LE) state, i.e., $k_{ET}^{LE}>k_{ET}^{CT}$.
- the values of $f_{LE}$ and $f_{CT}$ are closed to the values of $A_i$ describing contributions from different fluorescence emitting modes ( see Tables 1 and 2), e.g. for prodan in AcN: $f_{LE}=0.6$ and $A_2$(LE)=0.6, and $f_{CT}=0.4$ and $A_3$(CT)=0.35. While for laurdan in THF, the following results are:

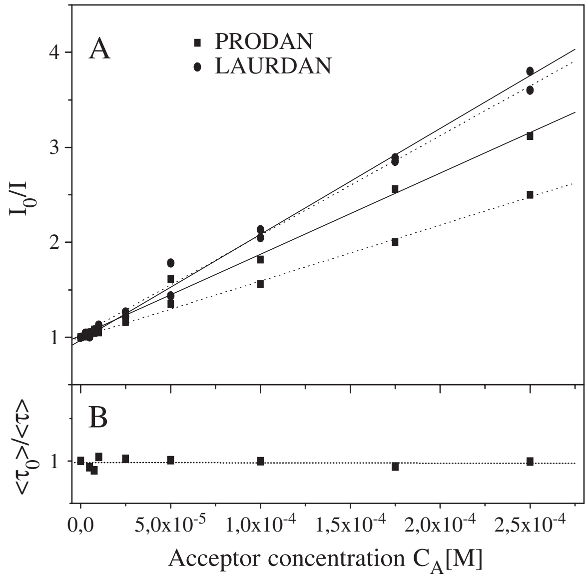

Fig. 4. A. Stern–Volmer plots of the fluorescence quenching of prodan and laurdan in THF (...) and AcN (—) using ORB as a quencher. B. The ratio of $\langle\tau_0\rangle/\langle\tau\rangle$ as function of quencher concentration for prodan-ORB system in THF.

Table 2

Stern–Volmer constants, $K_{SV}^{LE}$ and $K_{SV}^{CT}$, rate constants for fluorescence quenching, $k_{ET}^{LE}$ and $k_{ET}^{CT}$, and the fractional contributions of the emitting forms (LE and CT) to the total fluorescence intensity, $f_{LE}$ and $f_{CT}$, obtained from Eq. (2) for prodan+ORB and laurdan+ORB systems

| | Prodan | | Laurdan | |
|---|---|---|---|---|
| | THF | AcN | THF | AcN |
| $f_{LE}$ | 0.69 | 0.60 | 0.63 | 0.58 |
| $K_{SV}^{LE}$ [l mol$^{-1}$] | 11,228 | 9989 | 12,283 | 10,613 |
| $\tau_D^{LE}$ [ns] | 3.09 | 1.98 | 2.40 | 1.75 |
| $k_{ET}^{LE}$ [$\times10^{12}$ l mol$^{-1}$ s$^{-1}$] | 3.63 | 5.04 | 5.10 | 6.06 |
| $f_{CT}$ | 0.31 | 0.40 | 0.37 | 0.42 |
| $K_{SV}^{CT}$ [l mol$^{-1}$] | 11,227 | 10,456 | 12,283 | 10,615 |
| $\tau_D^{CT}$ [ns] | 5.46 | 3.84 | 3.93 | 3.68 |
| $k_{ET}^{CT}$ [$\times10^{12}$ l mol$^{-1}$ s$^{-1}$] | 2.05 | 2.72 | 3.10 | 2.88 |

$f_{LE}=0.63$ and $A_2(LE)=0.66$, and $f_{CT}=0.37$ and $A_3(CT)=0.3$. The differences are less than 10% and are in the error range of determination of $f_{LE}$, $f_{CT}$ and $A_i$. The observed compatibility between those values testify the correctness of the performed analysis.

### 3.4. Energy transfer

The experimental data show that the fluorescence quenching is a result of energy transfer, caused by dipole–dipole interactions between donor D and acceptor A molecules. According to Förster, the rate of energy transfer ($k_{ET}$) and the critical radius ($R_0$) can be expressed in quantities, accessible by spectroscopic measurements [20–22]:

$$k_{ET}=\frac{9000\ln 10\kappa^2\Phi_D^0}{128\pi^5n^4Nr^6\tau_D^0}J_{DA}(\tilde{\nu}) \tag{2}$$

and

$$R_0^6=\frac{9000\ln 10\kappa^2\Phi_D^0}{128\pi^5n^4N}J_{DA}(\tilde{\nu}), \tag{3}$$

where $\Phi_D^0$ and $\tau_D^0$ are the fluorescence quantum yield and lifetime of donor in absence of acceptor, respectively; $r$ is the distance between D and A molecules; $R_0$ is a critical radius for energy transfer; $n$ is a refractive index of the solvent; $\kappa$ is an orientation factor which takes into account the angle between the transition moments of the D an A molecules, which is equal $(2/3)^{1/2}$ for their random distribution; $N$ is the Avogadro's number. $J_{DA}(\tilde{\nu})$ is the spectral overlap integral between the donor emission and acceptor absorption spectra:

$$J_{DA}(\tilde{\nu})=\int_0^\infty \frac{I_{FD}(\tilde{\nu})\cdot\varepsilon_A(\tilde{\nu})}{(\tilde{\nu})^4}d\tilde{\nu}, \tag{4}$$

where $I_{FD}(\tilde{\nu})$is the spectral distribution of the donor fluorescence intensity normalized to the unit area in the wavenumber scale and $\varepsilon_A(\tilde{\nu})$is the molar extinction coefficient of the acceptor.

The values of spectral overlap integral $J_{DA}(\tilde{\nu})$ calculated according to Eq. (4) and $R_0$ data obtained from Eq. (3) are assembled in Table 3. The determined quantum yield of both probes in THF and AcN is listed in Table 3. too. As it can be seen from the obtained data, the values of fluorescence quantum yield and spectral overlap integral depend on polarity of the medium, and possess higher values for solutions of both dyes in AcN. This change is a result of increasing fluorescence emission of CT form of prodan and laurdan. Furthermore, it must be noted that the increased polarity of solvent prefers processes leading to creation of TICT conformers which effectively compete in emission of the LE fluorescence.

Table 3
Experimentally and theoretically obtained critical transfer distances, $R_0$, $R_0'$, $R_0''$, and values of $[C]_{1/2}$ for prodan+ORB and laurdan+ORB systems

| Donor | Solvent | $\Phi_D^0$ | $J_{DA}(\tilde{\nu})$ ($\times 10^{-11}$ cm$^6$ mol$^{-1}$) | $R_0$ (Å)[a] | $R_0'$ (Å)[b] | $R_0''$ (Å)[c] | $[C]_{1/2}$ ($\times 10^4$ mol l$^{-1}$)[d] |
|---|---|---|---|---|---|---|---|
| Prodan | THF | 0.30 | 0.927 | 127.8 | 132.8 | 131.2 | 1.76 |
| | AcN | 0.38 | 2.892 | 147.5 | 150.8 | 151.0 | 1.15 |
| Laurdan | THF | 0.28 | 0.849 | 124.5 | 162.6 | 164.0 | 0.90 |
| | AcN | 0.38 | 2.817 | 146.8 | 164.3 | 161.0 | 0.95 |

[a] Theoretically calculated using the Eq. (3).
[b] Theoretically calculated using the Eq. (5).
[c] Calculated using the Eq. (8).
[d] Determined from the Förster quenching theory.

As it follows from Table 3, the values of $R_0$ for prodan and laurdan ($R_0$ ~124.5–147.5 Å) increase with polarity of the medium, and indicate that dipole–dipole interaction is responsible for the resonance energy transfer mechanism. The value of the critical transfer distance, $R_0$, (obtained from Eq. (3)) has been calculated assuming that the distance between all the donor and acceptor pairs is constant, e.g., as for solid state or bichromophoric systems. It was shown [9], that for the solution Eq. (2) must be modified as:

$$k_{ET}=\frac{(R_0')^3}{(7.35\times 10^{-8})^3\tau_F^D}. \tag{5}$$

The $R_0'$ data calculated using Eq. (5) are inserted in Table 3, too. As it can be seen on analyzing the data of Table 3 the values of $R_0$ and $R_0'$ are in good conformity, and both indicate that the energy transfer occurs on the distance larger than the sum of collision radii, $R_D+R_A$. The sum of collision radii for the studied donor–acceptor pairs is about 4.5–7 Å.

The transfer of excitation energy from donor to acceptor causes a decrease of the quantum yield of the donor molecule. According to the Förster theory [20,21] the energy transfer efficiency, $E_T$, as well as the ratio, $\Phi_D/\Phi_D^0$, of fluorescence quantum yields depend on the reduced concentration, $\gamma_{DA}$, for donor overlapping as follows:

$$\frac{\Phi_D}{\Phi_D^0}=1-E_T=1-\sqrt{\pi}\gamma_{DA}\exp(\gamma_{DA})^2[1-\mathrm{erf}(\gamma_{DA})], \tag{6}$$

where erf ($\gamma_{DA}$) is the Gaussian error function defined by $\mathrm{erf}(x)=2\sqrt{\pi}\int_0^\infty \exp(-x^2)dx$, $\gamma_{DA}=C_A/C_{0A}$ is the reduced concentration for donor overlapping [20,21], where $C_A$ is the acceptor concentration and $C_{0A}$ is a critical concentration, which is related to the critical transfer distance $R_0$ as follows [23]:

$$C_{0A}=\frac{3000}{4\pi NR_0^3}. \tag{7}$$

The experimental values of $\Phi_D/\Phi_D^0$ and $E_T$ and their values predicted theoretically (using spectroscopicaly determined values of $\gamma_{DA}$ and Eq. (6)) are plotted as the function of acceptor concentration in Fig. 5. It can be seen that the empirical results are in good agreement with the predictions of the Förster theory. This conformity allows us to calculate the critical radius of energy transfer $R_0''$ in an independent way by means of the following formula [9]:

$$R_0''=7.35([C]_{1/2})^{-1/3}, \tag{8}$$

where $[C]_{1/2}$ is the acceptor concentration at which the relative fluorescence quantum yield of donor is reduced by half. The

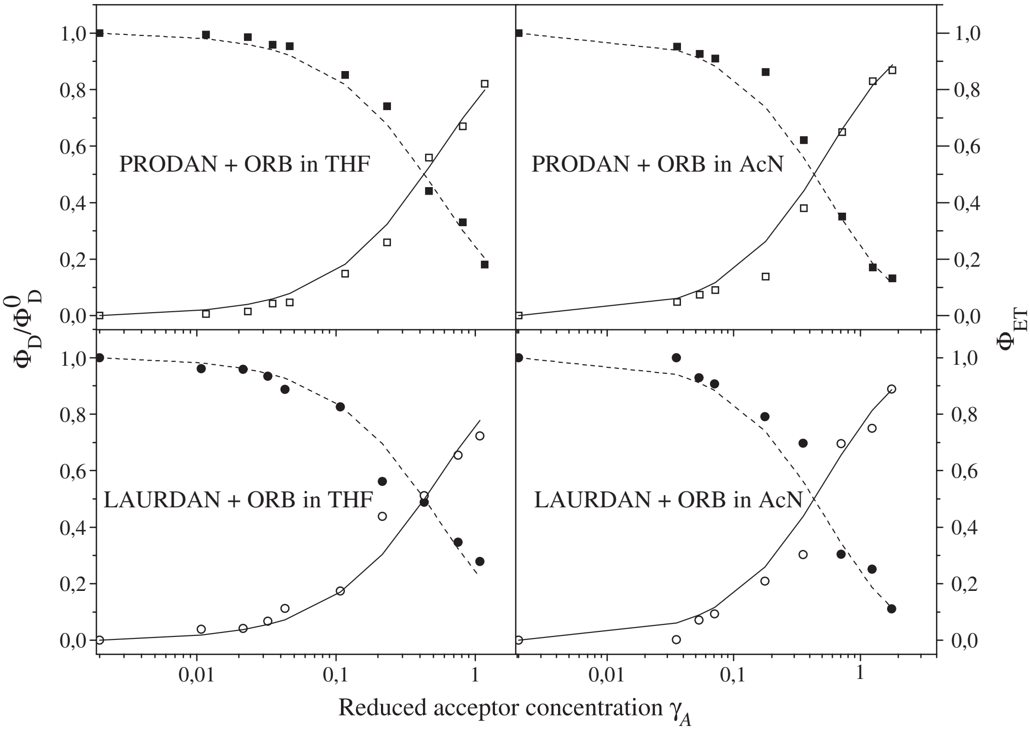

Fig. 5. Relative donor fluorescence quantum yield $\Phi_D/\Phi_D^0$ and energy transfer efficiency $E_T$ in presence of acceptor molecules dissolved in THF and AcN. The full and dashed curves are calculated from Eq. (6). The points represent the experimental results.

$[C]_{1/2}$ values of the acceptor concentration for all D–A pairs under study are summarized in Table 3. As it follows from Table 3, the values of $[C]_{1/2}$ are higher for laurdan-ORB in comparison to prodan-ORB. It indicates that the energy transfer is more efficient in case of prodan-ORB system irrespective of solvent polarity. The $R_0''$ values calculated using Eq. (8) are listed in Table 3, too. Analyzing $R_0$, $R_0'$ and $R_0''$ values determined using Eqs. (3), (5) and (8), follows that they are equal in the error range of their determination and they possess bigger value in more polar solvent AcN.

## 4. Conclusions

Our studies on fluorescence quenching of prodan and laurdan by ORB in THF and AcN bring us to following conclusions:

- The fluorescence quenching of prodan and laurdan by ORB shows different efficiencies. The emission of laurdan is quenched more effectively than that of prodan. We suppose that this finding is due to the different lengths of their acyl residues.
- The $R_0$ values for investigated donor–acceptor pairs range between 124.5 and 147.5 Å. It indicates that dipole–dipole interaction is responsible for the energy transfer mechanism.
- We are convinced that the modified Stern–Volmer relation is the proper one to study the quenching process of both systems. The correlation between $f_{LE}$, $f_{CT}$ and the values of $A_i$ describing contributions from different fluorescence modes speaks for the procedure which takes into account the noted spectral heterogeneity of solutions under study. The observed compatibility with results obtained using the standard Stern–Volmer model is a proof of properly of performed analysis.

## Acknowledgements

The authors express their gratitude to Prof. Piotr Kwiek and Dr Grzegorz Gondek for making the use of the fluorescence decay time setup possible, and to Dr Joanna Redzimska for her technical assistance during the manuscript revision.

## References

[1] M.R. Eftink, Fluorescence quenching: theory and applications, in: J.R. Lakowicz (Ed.), Topics in Fluorescence Spectroscopy: Principles, vol. 2, Plenum Press, New York, 1991, pp. 53–126.

[2] M.R. Eftink, Fluorescence quenching reactions: probing biological macromolecular structures, in: T.G. Dewey (Ed.), Biophysical and Biochemical Aspects of Fluorescence Spectroscopy, Plenum Press, New York, 1991, pp. 1–41.

[3] H.C. Cheung, Resonance energy transfer, in: J.R. Lakowicz (Ed.), Topics in Fluorescence Spectroscopy: Principles, vol. 2, Plenum Press, New York, 1991, pp. 127–176.

[4] P. Wu, L. Brand, Review: resonance energy transfer: methods and applications, Anal. Biochem. 218 (1994) 1–13.

[5] T.G. Dewey, Fluorescence energy transfer in membrane biochemistry, in: T.G. Dewey (Ed.), Biophysical and Biochemical Aspects of Fluorescence Spectroscopy, Plenum Press, New York, 1991, pp. 197–230.

[6] J.R. Lakowicz, Principles of Fluorescence Spectroscopy, Kulver Academic Publishers, New York, 1999.

[7] H.-W. Heldt, Plant Biochemistry and Molecular Biology, Oxford University Press, Oxford, 1997.

[8] O. Stern, M. Volmer, On the quenching time of fluorescence, Phys. Z. Sowjetunion 20 (1919) 183–188.

[9] N.J. Turo, Modern Molecular Photochemistry, Benjamin/Cummings, California, 1987.

[10] S.S. Lehrer, P.C. Leavis, Solute quenching of protein fluorescence, Methods Enzymol. 49 (1978) 222–236.

[11] M. Viard, J. Gallay, M. Vincent, O. Meyer, B. Robert, M. Paternostre, Laurdan solvatochromism: solvent dielectric relaxation and intramolecular excited-state reaction, Biophys. J. 73 (1997) 2221–2234.

[12] A.B.J. Parusel, W. Nowak, S. Grimme, G. Köhler, Comparative theoretical study on charge-transfer fluorescence probes: 6-propanoyl-2-(*N*,*N*-dimethylamino) naphthalene and derivatives, J. Phys. Chem., A 102 (1998) 7149–7156.

[13] V.I. Tomin, M. Brozis, J. Heldt, The red-edge effects in laurdan solutions, Z. Naturforsch. 58a (2003) 109–117.

[14] K.A. Kozyra, J.R. Heldt, J. Heldt, M. Engelke, H.A. Diehl, Concentration and temperature dependence of laurdan fluorescence in glycerol, Z. Naturforsch. 58a (2003) 581–588.

[15] M. Brozis, K.A. Kozyra, V.I. Tomin, J. Heldt, Inhomogeneous broadening of the electronic spectra of laurdan, J. Appl. Spectrosc. 69 (2002) 480–483.

[16] K.A. Kozyra, J.R. Heldt, G. Gondek, P. Kwiek, J. Heldt, Influence of DPPC liposome concentration on the fluorescence properties of prodan and laurdan, Z. Naturforsch. 59a (2004) 809–818.

[17] A. Synak, G. Gondek, P. Bojarski, L. Kułak, A. Kubicki, M. Szabelski, P. Kwiek, Fluorescence depolarization in the presence of excitation energy migration in partly ordered polymers films, Chem. Phys. Lett. 399 (2004) 114–119.

[18] K.A. Kozyra, J.R. Heldt, M. Engelke, H.A. Diehl, Phase transition affects energy transfer efficiency in phospholipid vesicles, Spectrochim. Acta, A 61 (2005) 1153–1161.

[19] B. Valuer, Molecular Fluorescence, Wiley-VCH Verlag, Weinheim, 2002.

[20] Th. Förster, Transfer mechanisms of electronic excitation, Discuss. Faraday Soc. 27 (1959) 7–17.

[21] Th. Förster, Transfer mechanism of electronic excitation energy, Radiat. Res. Suppl. 2 (1960) 326–339.

[22] J.B. Birks, Photophysics of Aromatic Molecules, Wiley, London, 1970.

[23] K.K. Pandey, T.C. Pant, Migration modulated donor–acceptor energy transfer in PMMA, J. Lumin. 47 (1991) 319–325.